Research Article

Nano Research
2021, 14(4): 1202–1209

ISSN 1998-0124 CN 11-5974/O4
https://doi.org/10.1007/s12274-020-3172-3

Hydrophobic ionic liquid-in-polymer composites for ultrafast, linear response and highly sensitive humidity sensing

Xuanliang Zhao[1], Kanglin Zhou[2], Yujia Zhong[1], Peng Liu[1], Zechen Li[1], Jialiang Pan[1], Yu Long[3], Meirong Huang[1], Abdelrahman Brakat[1], and Hongwei Zhu[1] (✉)

[1] *State Key Lab of New Ceramics and Fine Processing, School of Materials Science and Engineering, Tsinghua University, Beijing 100084, China*
[2] *Department of Electronic Engineering, Tsinghua University, Beijing 100084, China*
[3] *Department of Mechanical Engineering, University of California, Berkeley, USA*

Received: 19 July 2020 / **Revised:** 5 September 2020 / **Accepted:** 9 October 2020

ABSTRACT

Traditional ionic liquids are sensitive to humidity but with long response time and nonlinear response. Pure liquid-state ionic liquids are usually hard for dehydration which have ultralong response time for humidity sensing. The immobilization of ionic liquids provide a possible way for high performance humidity sensing. Hydrophobic materials and structures also promised faster response in humidity sensing, because of easier desorption of water. In this work, we prepared flexible humidity sensitive composites based on hydrophobic ionic liquid and polymer. The combination of hydrophobic ionic liquid with hydrophobic polymer realized linear response, high sensitivity with low hysteresis to humidity. By adjusting the ratio of ionic liquid, not only the impedance but also the hydrophobicity of composite could be modulated, which had a significant influence on the humidity sensing performance. The morphology and microstructure of the material also affected its interaction with water molecules. Due to the diverse processing methods of polymer, highly transparent film fabricated by spinning-coating and nanofibrous membrane fabricated by electrospinning could be prepared and exhibited different response time, which could be used for different application scenarios. Especially, the fibrous membrane made with electrospinning method showed an ultrafast response and could distinguish up to 120 Hz humidity change, due to its fibrous structure with high specific surface area. The humidity sensors with ultrafast, linear response and high sensitivity showed potential applications in human respiratory monitoring and flexible non-contact switch. To better show the multifunction of ionic liquid-polymer composite, as a proof of concept, we fabricated an integrated humidity sensitive color change device by utilizing lower ionic liquid content composite for sensing in the humidity sensing module and higher ionic liquid content composite as the electrolyte in the electrochromic module.

KEYWORDS

ionic liquid, flexible humidity sensing, ultrafast response, hydrophobic

1 Introduction

Flexible sensors have attracted lots of research interests for their potential applications in soft robotics [1, 2], electronic skins [3–5] and human healthcare [6–8]. Compared with traditional rigid sensors, flexible sensors can be attached to different surfaces so that they can be more suitable used in wearable electronics. Moisture is one of the most vital factors for the environment and living beings. Monitoring humidity plays a vital role in many areas, such as agriculture, medicine and electronics industries and health monitoring [9]. A lot of materials such as ceramics [9], polymers [10] and graphene [11, 12] have been used in developing humidity sensors. However, it remains a significant challenge to fabricate humidity sensors with a complete set of desirable properties: high sensitivity, excellent linearity, fast response time, low hysteresis, and so on [13]. Meanwhile, developing flexible humidity sensors in simple ways, but with high performance is our pursuit.

Ionic liquids (ILs) are a class of molten salts formed by the combination of organic cations and organic or inorganic anions. Similar to liquid metals, ILs are flowable and conductive at room temperature. Besides, ILs have many unique properties such as low volatility, high ionic conductivity, excellent thermal stability, low flammability and low toxicity [14]. Because of their attractive properties, the ILs have been developed for diverse applications [15], such as electrodes and electrolytes in lithium and sodium batteries [16, 17], electrolytes in supercapacitors [18, 19], catalysis [20, 21], sensors [22–24], *etc.* The conductivity of pure ILs was reported to change with water content [25] because of the viscosity change. This provided the possibility for the application of ILs in humidity sensing. Liquid-state heterojunction sensor fabricated with IL and Galinstan was sensitive to humidity change, but the response time lasted for hours [26]. When liquid-state IL was mixed with moisture, it would be harder for them to be separated compared with solid-state materials and moisture. This caused the most serious problem of ILs in humidity sensing: long response time. The immobilization of ionic liquid with solid materials can change the interaction between water molecular and liquid into the interaction between water molecular and solid, which will improve the response time. Wang and his co-workers developed an ionogel humidity sensor based on IL which was immobilized on SiO_2 particles

Address correspondence to hongweizhu@tsinghua.edu.cn

[27], showing fast-response to humidity change. But it lacked flexibility. Polymerized ILs were promising materials for immobilizing ILs which remained the specific properties of ILs. The solid-state poly(ionic liquid)s [28] was reported to act as humidity sensing film with good flexibility, while complex polymerization reaction was needed. Recently, Fernandes and his co-workers developed a humidity sensor based on hydrophilic ionic liquid which was mixed with polymer [29]. But the response time was still at several minutes' level. Thus, fabricating flexible and high-performance (especially ultrafast response) IL-based humidity sensor in a simple way remains a problem. At the same time, multifunctional devices based on ILs were rarely reported.

In this work, we immobilized hydrophobic ILs with polymer and prepared a flexible humidity sensitive composite based on IL (1-ethyl-3-methylimidazolium bis(trifluoromethylsulfonyl) imide, $[EMI]^+$ $[TFSI]^-$) and polymer (poly(vinylidene fluoride-co-hexafluoropropylene), P(VDF-HFP)). Hydrophobic materials and structures have been proved a good choice to achieve faster response [30, 31] and lower wet hysteresis [32] in humidity sensing. The combination of hydrophobic IL and hydrophobic polymer provided a facile method to realize ultrafast response. Owing to the polymer matrix, diverse but easy processing methods could be used as well. Different sensor types of transparent film and nanofibers were respectively fabricated with spinning-coating and electrospinning method. All the sensors showed a linear response with high sensitivity (−0.70%/%RH), minimal wet hysteresis and an ultrafast response to humidity change. In particular, the nanofibrous sensor could detect the frequency of 120 Hz humidity change. Besides, to better show the multifunction of ionic liquid-polymer composite, as a proof of concept, we fabricated an integrated humidity sensitive color change device based on IL and polymer composite by adjusting the content of IL in different functional modules.

2 Results and discussion

2.1 Preparation and structure of the humidity sensitive composite

The flexible humidity sensitive composite consists of two components: P(VDF-HFP), which acts as the polymer matrix and $[EMI]^+$ $[TFSI]^-$ as the IL (Fig. 1(a)). Both $[EMI]^+$ and $[TFSI]^-$ are very hydrophobic ions [17]. P(VDF-HFP) which has lots of C-F bonds is also a kind of hydrophobic polymer. Compared with PVDF, the CF_3 pendant in P(VDF-HFP) can cause more steric hindrance effect and can provide more free volume for mobile ions, which is beneficial for raising the conductivity of the composite. The polymer and the IL were both dissolved in an organic solvent like acetone or dimethylformamide (DMF) and then were sufficiently stirred to get a uniform solution. After evaporating the solvent, the humidity sensitive composite was obtained. The conductivity of the composite could be significantly adjusted by changing the content of the IL in the composite. As shown in Fig. 1(b), the complex plots of the composites with the IL content below 16.7% were straight lines, which meant that the composites were highly insulative. The complex plots of the composites with the IL content above 23.1% were composed of a semicircle and a shot line. With the increase of the IL content, the diameter of the semicircle decreased from tens of megohm to tens of kiloohm.

The polymer was known to have excellent molding properties and can be formed into various shapes through extrusion, injection, spinning process, *etc*. The polymer and the IL which dissolved in acetone could be spinning-coated to fabricate highly transparent film (Fig. 1(c)). The transparent film was self-supporting and quite flexible. The transparent film could be formed in a large area (~ 20 cm^2) at one time (Fig. 1(d)). What's more, the transmittance of the film in the visible wavelength

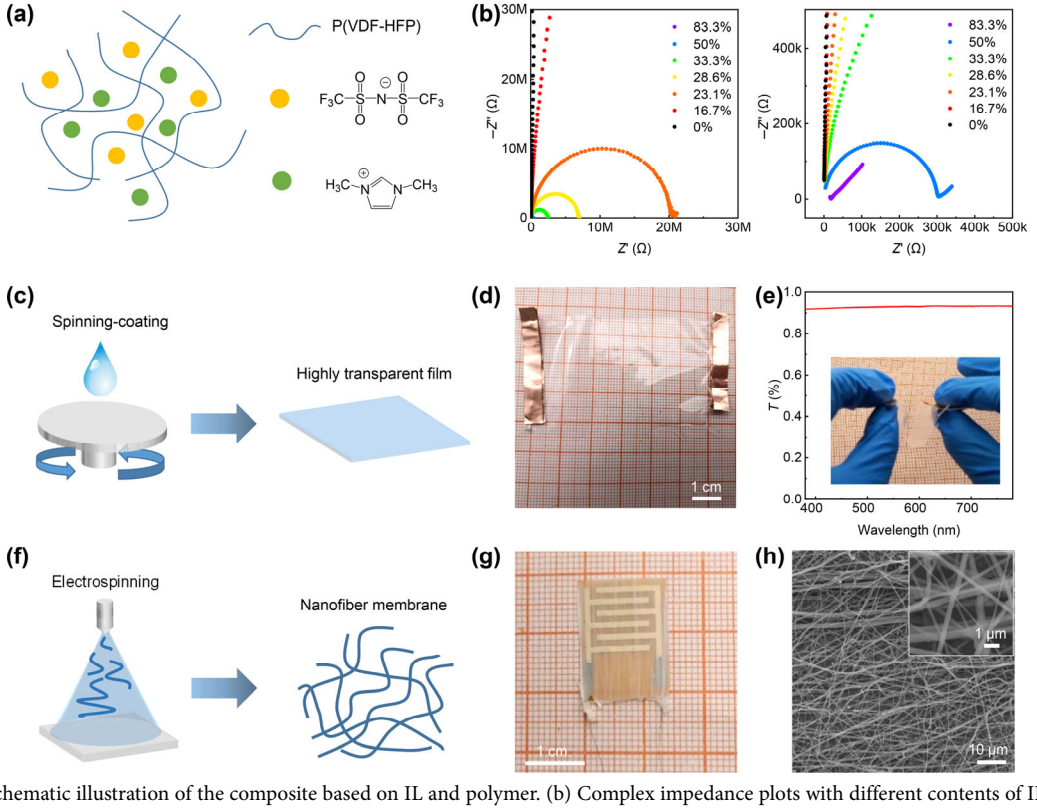

Figure 1 (a) Schematic illustration of the composite based on IL and polymer. (b) Complex impedance plots with different contents of IL obtained from 40 Hz to 10 MHz. (c) Schematic illustration of highly transparent spinning-coated film. (d) Photograph of the spinning-coated film. (e) UV–vis absorption spectrum of the spinning-coated film. Inset shows the photograph of a bent film. (f) Schematic illustration and (g) photograph of the electrospun membrane. (h) SEM images of electrospun nanofibers.

range was above 93% (Fig. 1(e)).

Electrospinning is an important method which can be used to fabricate polymer nanofiber membrane (Fig. 1(f)). Due to the low shear viscosity and low boiling point of acetone, acetone was not suitable for stable electrospinning. Thus, DMF was used as the solvent of the polymer and the IL. By electrospinning, composite nanofibers of P(VDF-HFP) and $[EMI]^+$ $[TFSI]^-$ were successfully fabricated (Fig. 1(g)). The diameters of fibers were around several hundred nanometers (Fig. 1(h)). The fibers connected with each other and formed conductive networks. Due to the point contact of the fibers, the impedance of the electrospun membrane was much higher than the spinning-coated transparent film. In order to reduce the impedance of the device, flexible polyimide (PI) substrate with interdigitated electrodes was used to collect the nanofibers during electrospinning.

2.2 Humidity sensing

As for a humidity sensor, the sensitivity, linearity and response time are quite essential parameters. Meanwhile, wet hysteresis often exists due to the difference of hygroscopic and dehumidifying processes. Yet as a humidity sensor, wet hysteresis should be as small as possible to improve the accuracy of humidity sensing.

The content of 40% $[EMI]^+$ $[TFSI]^-$ in the composite was chosen to fabricate both spinning-coated film and the electrospun nanofiber membrane to act as humidity sensors. Experimentally, it is worth noting that the low concentration of IL would lead to very large impedance and cause inconvenience in the humidity test. Meanwhile, the high concentration of IL sample would make it not suitable for electrospinning because of its high conductivity.

Good linearity has a vital influence on the sensor calibration and data processing [33]. However, lots of humidity sensors reported a lack of linearity response to the humidity change. The impedance response of humidity sensors made by P(VDF-HFP) and $[EMI]^+$ $[TFSI]^-$ showed very good linearity to the humidity change (10%–80%), whether the sensor was a spinning-coated transparent film (Figs. 2(a) and 2(b)) (the linearly dependent coefficient, $r = -0.9997$) or electrospun nanofiber membrane (Figs. 2(c) and 2(d)) ($r = -0.9976$). The impedance changes of the humidity sensors during humidity increase process and humidity decrease process were almost located on the same line, which meant that the wet hysteresis was not obvious. The sensitivity of the humidity sensor was defined as $S = (Z - Z_{50\%})/(Z_{50\%} \times \Delta H)$ ($Z_{50\%}$ is defined as the impedance at the humidity of 50%RH). The sensitivity of the spinning-coated film was calculated as −0.70%/%RH, and that of the electrospun film was −0.79%/%RH.

The response time is also an important performance parameter of a humidity sensor. To test the ultrafast humidity response, the environment with ultrafast humidity change should be created. The common methods to control the humidity include pumping the mixed gas of different proportions of dry air and wet air or using saturated salt solutions. However, it takes a little long time to reach the equilibrium humidity with these methods. Therefore, in our work, a chopper was used to control the humidity change and test the ultrafast response time. The high humidity gas was introduced through a tube, and wet airflow was intercepted periodically by the chopper (Fig. 3(a)). Consequently, this could create a systematically and rapidly changing humidity environment. Meanwhile, a resistance-to-voltage conversion circuit module was used to convert impedance changes of the sensor to voltage changes, which could be further recorded by an oscilloscope. It can be noted that almost two factors were found to have great influences on the response

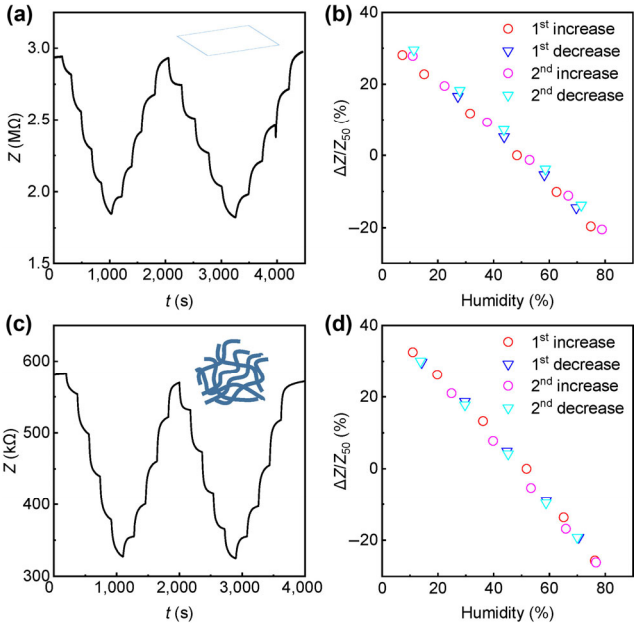

Figure 2 (a) Time-resolved impedance variation of the spin-coated film with step changes of humidity. (b) Impedance variation of the spin-coated film with humidity. (c) Time-resolved impedance variation of the electrospun membrane with step changes of humidity. (d) Impedance variation of the electrospun membrane with humidity.

time of the humidity sensor, such as the content of the ionic liquid and the morphology of the membrane.

The composite that contained a very low concentration (< 16.7%) of IL was not suitable to sense humidity because of its overlarge impedance. The composite with high concentration (83.3%) of IL could only be fabricated into a transparent film using the spinning-coating method. The composite with medium concentration (40.0%) of IL could be both spinning-coated and electrospun. However, even under 10 Hz humidity change, the spinning-coated film containing 83.8% IL could not distinguish the fast humidity change (Fig. 3(b)). For the spinning-coated film containing 40.0% IL, the frequency of humidity change below 30 Hz could be distinguished (Fig. 3(c)). This could mainly be attributed to the differences between the hydrophilicity of the films. The contact angle of the film which contained 40.0% IL was around 95° (Fig. S1(a) in the Electronic Supplementary Material (ESM)), while that of the film which contained 83.3% IL was 57° (Fig. S1(b) in the ESM). It was observed that increasing of the IL content would increase the hydrophilicity of the membrane. If a material was too hydrophilic, it would be more difficult to dehydrate when the humidity was decreased. This would cause long recovery time of humidity sensing. On the contrary, water microdroplets tended to be standalone rather than aggregate into larger units on hydrophobic surface, which has been proved in our previous work [30]. The standalone microdroplets could provide larger evaporation area compared with gathered droplets, so that water molecules could more easily depart from the absorbed surface when humidity decreased. However, much lower concentrations of IL would cause the increase of impedance, which would further make it difficult for impedance measurement. Meanwhile, if a material was too hydrophobic, it would be hard to act with water molecules. In this case, water would cause little effect on this material, and the material would be less sensitive to humidity change. Thus, proper concentration of IL was important for fast humidity response. The medium concentration (~ 40.0%) of IL had enough hydrophobicity and proper impedance, which was suitable for fast humidity response.

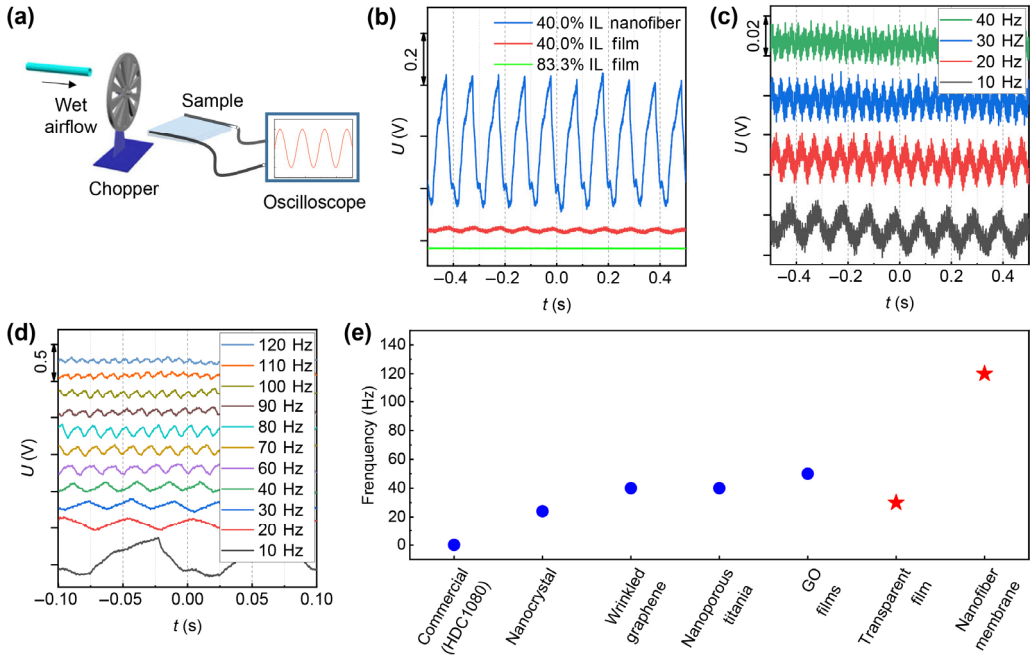

Figure 3 (a) Schematic illustration of the test setup for the response speed of humidity sensors. (b) Responses of 40% IL nanofiber, 40% IL film and 83.3% IL film to humid air flow at 10 Hz. (c) Responses of 40% IL film to a humid air flow from10 to 40 Hz. (d) Responses of 40% IL nanofiber to a humid air flow from 10 to 120 Hz. (e) Summary of the performances of some reported ultrafast humidity sensors.

The morphology of the membrane also played an essential role in fast response to humidity change. The nanofiber membrane containing 40.0% IL had a fast response time of humidity and good ability to detect highly frequent humidity change. When the humidity change frequency was 10 Hz, the response of the nanofibrous membrane was much more distinct compared with that of the spinning-coated film (Fig. 3(b)). As shown in Fig. 3(d), even 120 Hz of humidity change could be distinguished by the nanofibrous membrane. Remarkably, this was one of the highest frequencies which could be achieved (Fig. 3(e) and Table S1 in the ESM) among the reported ultrafast humidity sensors [30, 34–36]. It was evident that the nanofiber structure had a very high specific surface area, and more surfaces were exposed to the environment as well. Therefore, the nanofibers could have better interaction with water molecules, and this would cause an ultrafast response to humidity change.

Complex impedance plots were usually used to study the mechanism of ionic conductive type humidity sensors [27, 28, 37, 38]. The complex impedance plots of the IL-based sensor were tested from 40 Hz to 10 MHz at different RH levels by Agilent 4294A. All the complex impedance plots at different RH levels were similar, which were composed of an arc and a line (Fig. S2(a) in the ESM). It is also worth noting that the impedance mainly was composed of two parts, the intrinsic impedance of the films and ion diffusion impedance (the Warburg impedance). The impedance plots could be fitted to an equivalent circuit with the Zsimpwin software (Fig. S2(b) in the ESM). The equivalent circuit was composed of four elements: R_s, R_1, CPE and W. R_s is closely related to the surrounding region of the electrode. R_1 represents the bulk resistance of the sensing film and CPE is related to the influence of polarization in the sensing film. Warburg impedance (Zw) reflects the effect of diffusion process of ions or charge carriers. The change of element R_1 and W played the most important role in humidity change in the equivalent circuit (Figs. S2(c)–S2(f) in the ESM). The change of R_1 and W of ILs-polymer composite was closely related to the change of ionic conductivity. The water molecules could be adsorbed to the surface of the polymer and produce free protons (H^+) ionized from H_2O. With the increase of humidity, more water molecules would be absorbed to produce more ionized H^+. This led to an increase in movable ions and the increase of film conductivity.

Therefore, the realization of ultrafast humidity sensing performance was illustrated in Fig. 4. The conductivity change of the IL-polymer composite was attributed to the ionization of the adsorbed water. At molecular scale, the hydrophobic ionic liquid and hydrophobic polymer were used to form hydrophobic composite, which was favorable for water molecule desorption when humidity decreased. The immobilization of ionic liquid by polymer changed the interaction between water molecular and liquid into the interaction between water molecular and solid, which could also improve the response speed. At microscale, by adjusting microstructure of the composite, nanofibrous structure could be achieved, which could provide high specific surface area. These factors synergistically realized the ultrafast humidity sensing of IL-based composite.

2.3 Applications of the humidity sensor

The flexible humidity sensor fabricated by P(VDF-HFP) and $[EMI]^+$ $[TFSI]^-$ showed good sensitivity to humidity change with excellent linearity, low wet hysteresis and fast response-ability. Hence it can be used in wearable devices.

Respiration is an important physiological activity for human. The monitoring of respiration has great importance for human health. For example, the monitoring of respiration during exercise can reduce the risk of excessive movement. And the monitoring of respiration during sleep can help to evaluate sleeping quality and timely discover some sleep apnea syndromes. Due to the high humidity of the gas that human exhaled, respiratory can be monitored by humidity sensors. The IL-based flexible sensor was attached to the philtrum of a volunteer (Fig. 5(a) inset). The normal breathing of a volunteer was first detected (Fig. 5(a)), and the respiratory rate was around 18 times per minute (12–20 times per minute are within normal limits). The situation of rapid panting, which may happen when asthma

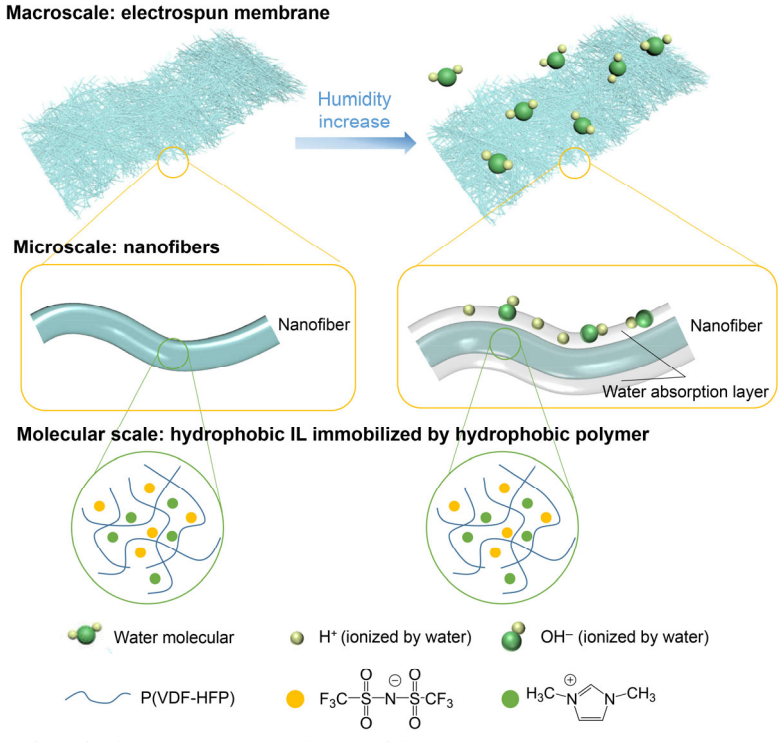

Figure 4 Schematic illustration of ultrafast humidity sensing mechanism of the IL-based composite.

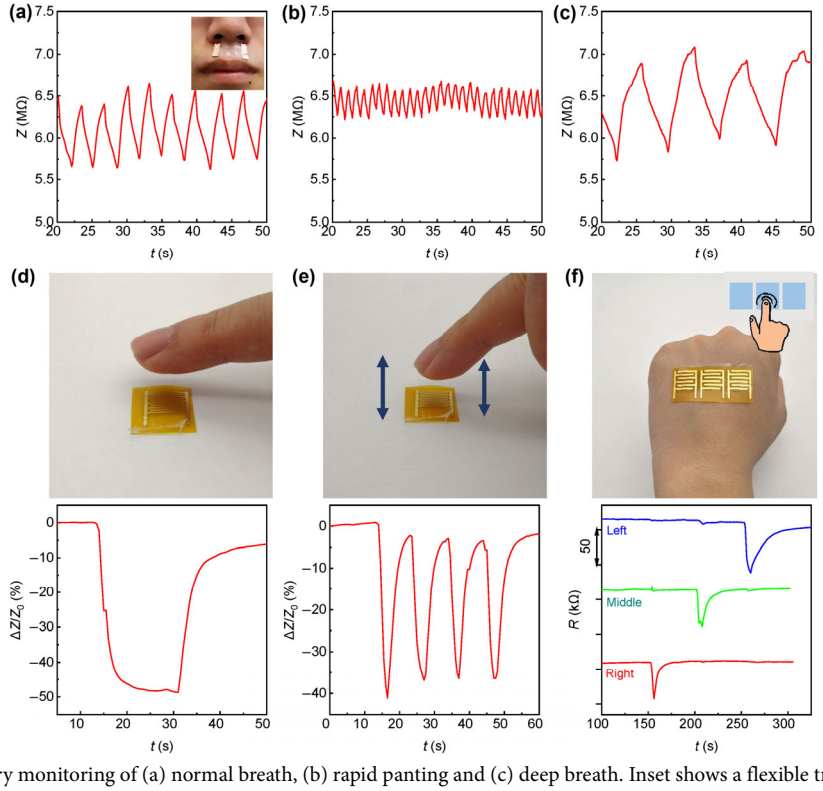

Figure 5 Human respiratory monitoring of (a) normal breath, (b) rapid panting and (c) deep breath. Inset shows a flexible transparent sensor attached to the philtrum. (d)–(f) Non-contact switches: (d) Photograph and impedance change of the sensor when the finger approached the sensor. (e) Photograph and impedance change of the sensor when the finger tapped and lifted. (f) Photograph and impedance change of 1×3 non-contact switch array when the finger approached the left, middle and right part of the array.

occurs or after strenuous exercise was also simulated. The respiratory rate reached around 55 times per minute, while the amplitude of impedance change was small (Fig. 5(b)). When the volunteer breathed deeply, the impedance changed larger than that of normal breath, and the respiratory rate was 8 times per minute (Fig. 5(c)). Different breathing conditions could be monitored and distinguished with our flexible humidity sensor. Furthermore, the transparent film has less influence on aesthetics because of its high transparency.

Another application is for a non-contact switch. Contact switches may cause cross-infection of bacteria or virus, while non-contact switches can reduce this risk. The water evaporation from the skin can change the humidity near the skin. This feature can be used to achieve non-contact control by using the humidity sensor. As shown in Fig. 5(d), when the fingertip approached the humidity sensor, it would cause impedance

decrease. When the finger stayed near, the impedance decreased and formed a platform region. When quickly tapped and lifted a finger, falling peaks of impedance would appear (Fig. 5(e)). Furthermore, a non-contact switch array composed of several humidity sensors was fabricated with one-step spinning-coating or electrospinning method. The flexible non-contact switch array could be attached to the skin. Then, as the finger approached the left, middle or right part of the array, the sensor at the corresponding position could record the position information of the finger and realize different signal inputs (Fig. 5(f)).

2.4 Integrated humidity sensitive color change device

The versatility of ionic liquid-polymer composites provided them with multifunctional applications in various fields. But traditionally, the applications of ionic liquids were relatively independent of each other. As a multifunctional material, it makes great sense to develop a device which combines sensing, displaying, energy storing and other functions. When a multifunctional device is fabricated with the same materials system, it can use the same processing technology and equipment, which is beneficial for simplifying processing and reducing the cost. In addition, multifunctional devices using the same materials system makes it easier in recycling and treatment after the failure of devices, which is beneficial to environment protection.

Visualization of the sensors can provide people with directly readable signals and more friendly information interaction. Humidity sensitive color change device has potential applications in humidity-responsive display and visualization of humidity sensing [35, 39, 40]. Traditional colorimetric humidity sensing materials like cobalt salts, $CuSO_4$, *etc.* had limited colors to change and the humidity at which the color would change was hardly to be adjusted. Fernandes, et al. developed a colorimetric device based on the water absorption and dehydration of Ni^+ in the IL of $[Bmim]_2[NiCl_4]$ [41]. Since the color change property mainly relied on Ni^+, it had the same drawbacks as the traditional colorimetric humidity sensing materials. In the composite system of P(VDF-HFP) and ionic liquid, high concentration of IL would lead to high ionic conductivity, which is suitable to act as an electrolyte. In previous reports [42, 43], P(VDF-HFP) and the ionic liquid composite was used in fabricating flexible electrochromic devices. This provided a new strategy to develop a humidity sensitive color change device based on the material system of ionic liquid-polymer composites.

Here, P(VDF-HFP) and $[EMI]^+$ $[TFSI]^-$ was used to fabricate the humidity sensitive color change device which was composed of the humidity sensing module and electrochromic module. The composites with different concentrations of IL played different roles in the functional modules. The composite with medium concentration (40.0%) of IL was used as humidity sensing material in the sensing module, and the composite with high concentration (83.3%) of IL acted as the electrolyte in the electrochromic module (Fig. 6(a)). Regarding the electrochromic part, dimethyl ferrocene (dmFc) and heptyl viologen bis-(trifluoromethylsulfonyl)imide ($HV(TFSI)_2$) were mixed with P(VDF-HFP) and $[EMI]^+$ $[TFSI]^-$ and acted as electrochromic materials. Two pieces of flexible indium tin oxide (ITO)-coated polyethylene terephthalate (PET) films served as the transparent conductive electrode and also separated the humidity sensing part from the electrochromic part. Besides, a circuit was designed to transfer the impedance change of the sensing part which varied with humidity into the input voltage change of the electrochromic part (Fig. 6(b)). The whole device was integrated through the layer-by-layer assembly process and was quite flexible (Fig. 6(c)). The UV–vis spectra of the device at various input voltages which were applied to the electrochromic part were illustrated in Fig. 6(d). When the voltage was over 0.6 V, the absorption peaks at around 400 and 600 nm appeared.

Generally, the impedance of the humidity sensing part decreased when the humidity of the environment increased. Then, the input voltage of the comparison circuit would increase. Meanwhile, it can be seen that the output voltage of the conversion circuit would be at a high level when the input voltage exceeded the comparison voltage. Consequently, this would cause the color change of the electrochromic part. After the humidity recovered to the original state, the output voltage of the conversion circuit would be at a low level (Fig. 6(e)); therefore, the color of the device would fade. The photographs of the integrated humidity sensitive color change device at low humidity level (light colored), high humidity level (deep colored) and after humidity recovered to low humidity level (color faded) were shown in Figs. 6(f)–6(h). In fact, the comparison voltage of the comparison circuit could be controlled, hence the humidity at which the color would change could be adjusted. Furthermore, other electrochromic materials with different colors could also be mixed in the IL-based electrolyte, so that the device had the potential to realize more color changes.

3 Conclusions

In this work, flexible humidity sensitive composites based on hydrophobic P(VDF-HFP) and $[EMI]^+$ $[TFSI]^-$ were fabricated by a facile approach utilizing various polymer molding methods. The composite showed a linear response to the humidity change with high sensitivity and small wet hysteresis. The spinning-coated film could response to 30 Hz humidity change, and the 120 Hz of humidity change could be distinguished by the electrospun membrane, which was one of the highest humidity change frequencies that had ever been reported. The flexible humidity sensors could be used in applications in human respiratory monitoring and flexible non-contact switch. As a proof of concept, a P(VDF-HFP) and $[EMI]^+$ $[TFSI]^-$ composite based integrated humidity sensitive color change device was also fabricated, which provided new ideas for building new humidity-sensitive color-changing devices.

4 Methods

Materials. The P(VDF-HFP) (No. 427187) was purchased from Sigma-Aldrich and the 1-ethyl-3-methylimidazolium bis(trifuoromethylsulfonyl)imide (EMITFSI) was purchased from Energy Chemical.

Fabrication of the flexible transparent humidity sensor. Certain amounts of P(VDF-HFP) and $[EMI]^+$ $[TFSI]^-$ were dissolved in acetone. After 4-h stirring, the mixture solution was spinning-coated on the substrate to obtain a transparent film.

Fabrication of the nanofibrous humidity sensor. Certain amounts of P(VDF-HFP) and $[EMI]^+$ $[TFSI]^-$ were dissolved in DMF. As for the electrospinning process, a voltage of 15 kV was applied to the syringe needle, and the collector was set to rotate at the speed of 100 r/min. The electrospun nanofibers were collected with PI substrate on which interdigital electrodes were deposited.

Fabrication of integrated humidity sensitive color change device. The integrated humidity sensitive color change device was divided into two parts: the humidity sensitive part and the

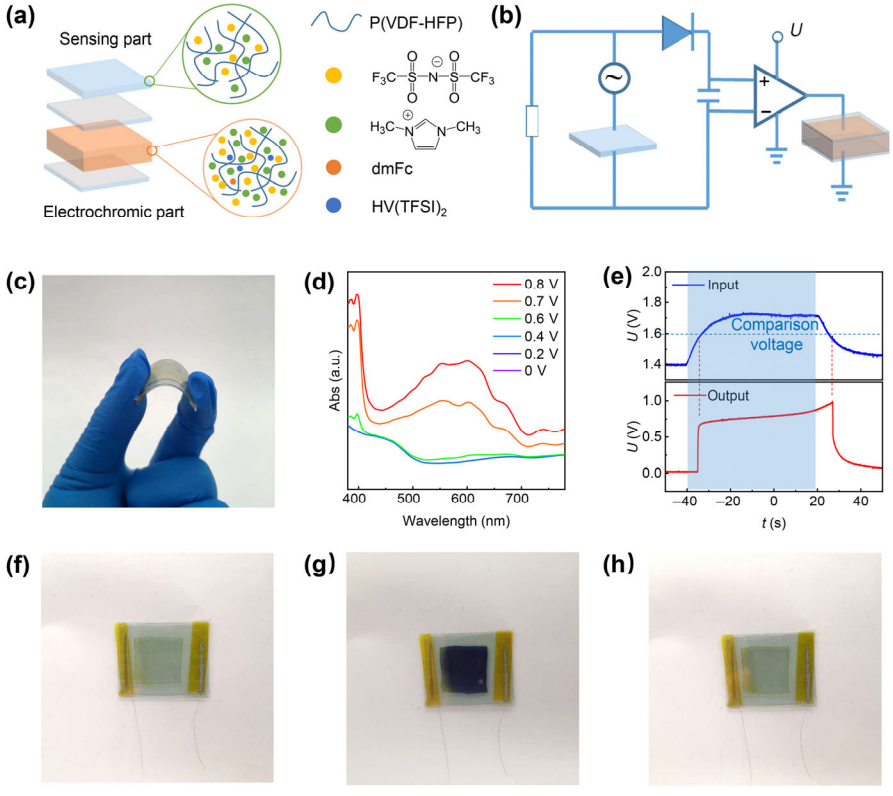

Figure 6 Integrated humidity sensitive color change device. (a) Schematic illustration of the device. (b) Schematic of the circuit layout. (c) Photograph of a bent device. (d) UV–vis spectra of the device when varied voltages applied on the electrochromic part. (e) Input and output voltage changes of the comparison circuit when humidity increased and then recovered. (f)–(h) Photographs of the devices at (f) low humidity level, (g) high humidity level and (h) after humidity recovered to low humidity level.

electrochromic part. The electrochromic part was fabricated as reported previously [42]. The electrochromic material $HV(TFSI)_2$ was prepared by an anion exchange reaction between heptyl viologen dibromide ($HV(Br)_2$) and lithium bis(trifluoromethylsulfonyl)imide (LiTFSI). $HV(TFSI)_2$, dmFc, P(VDF-HFP) and $[EMI]^+$ $[TFSI]^-$ (weight ratio: 3:1:12:60) were dissolved in acetone. The obtained solution was molded in a glass petri dish and dried to form solid-state electrolyte of the electrochromic part. The electrolyte was then sandwiched between two pieces of ITO-coated PET to form the electrochromic part. Finally, 40% content of IL solution of (P(VDF-HFP) and $[EMI]^+$ $[TFSI]^-$) was spinning-coated on the top of electrochromic part to act as the humidity sensing part.

Measurement of humidity sensing performance. The impedance of the humidity sensor was tested by Keysight E4980AL with 50 Hz, 2 V alternating voltage. The humidity sensing test was conducted by placing the sensor in a gas chamber. Different proportions of dry N_2 and wet N_2 (bubbled in deionized water) were mixed and then pumped into the chamber. The humidity in the gas chamber was adjusted by controlling the flow rates of the dry N_2 and the wet N_2 and calibrated with a commercial humidity sensor (CEM DT-83). The rapid humidity response test was conducted by using a chopper. Different frequencies of the chopper were set, and then wet N_2 passed the chopper; thus, different frequencies of humidity change were produced. The wet N_2 flow with a humidity of 90.2%RH and the gas flow rate of 25 mL/min was used. The humidity of the environment was 56.6%RH. A resistance-to-voltage conversion circuit module was used to convert impedance changes of the sensor to voltage changes and then the voltage changes were recorded by an oscilloscope (HDO6000A High Definition Oscilloscopes, Teledyne LeCroy Inc.).

Characterizations. The microstructure of the electrospun nanofibers was characterized by scanning electron microscopy (SEM) (Zeiss Merlin Compact). The ultraviolet-visible absorption spectra were measured by a spectrophotometer (Agilent Cary 5000).

Acknowledgements

This work was supported by the National Key Research and Development Program of China (No. 2017YFB1104300) and the National Natural Science Foundation of China (No. 51672150).

Electronic Supplementary Material: Supplementary material (the contact angle measurements, complex impedance plots and the comparison table of some reported ultrafast humidity sensors) is available in the online version of this article at https://doi.org/10.1007/10.1007/s12274-020-3172-3.

References

[1] Xie, M. Y.; Hisano, K.; Zhu, M. Z.; Toyoshi, T.; Pan, M.; Okada, S.; Tsutsumi, O.; Kawamura, S.; Bowen, C. Flexible multifunctional sensors for wearable and robotic applications. *Adv. Mater. Technol.* **2019**, *4*, 1800626.

[2] Abels, C.; Mastronardi, V. M.; Guido, F.; Dattoma, T.; Qualtieri, A.; Megill, W. M.; De Vittorio, M.; Rizzi, F. Nitride-based materials for flexible MEMS tactile and flow sensors in robotics. *Sensors* **2017**, *17*, 1080.

[3] Wang, X. D.; Dong, L.; Zhang, H. L.; Yu, R. M.; Pan, C. F.; Wang, Z. L. Recent progress in electronic skin. *Adv. Sci.* **2015**, *2*, 1500169.

[4] Chen, D.; Pei, Q. B. Electronic muscles and skins: A review of soft sensors and actuators. *Chem. Rev.* **2017**, *117*, 11239–11268.

[5] Liu, C. Y.; Huang, N. G.; Xu, F.; Tong, J. D.; Chen, Z. W.; Gui, X. C.; Fu, Y. L.; Lao, C. S. 3D printing technologies for flexible tactile

sensors toward wearable electronics and electronic skin. *Polymers* **2018**, *10*, 629.
[6] Tran, Q. T.; Lee, N. E. Flexible and stretchable physical sensor integrated platforms for wearable human-activity monitoring and personal healthcare. *Adv. Mater.* **2016**, *28*, 4338–4372.
[7] Yang, Y. R.; Gao, W. Wearable and flexible electronics for continuous molecular monitoring. *Chem. Soc. Rev.* **2019**, *48*, 1465–1491.
[8] Yang, H. G.; Xue, T. Y.; Li, F. Y.; Liu, W. T.; Song, Y. L. Graphene: Diversified flexible 2D material for wearable vital signs monitoring. *Adv. Mater. Technol.* **2018**, *4*, 1800574.
[9] Farahani, H.; Wagiran, R.; Hamidon, M. N. Humidity sensors principle, mechanism, and fabrication technologies: A comprehensive review. *Sensors* **2014**, *14*, 7881–7939.
[10] Najeeb, M. A.; Ahmad, Z.; Shakoor, R. A. Organic thin-film capacitive and resistive humidity sensors: A focus review. *Adv. Mater. Interfaces* **2018**, *5*, 1800969.
[11] Tulliani, J. M.; Inserra, B.; Ziegler, D. Carbon-based materials for humidity sensing: A short review. *Micromachines* **2019**, *10*, 232.
[12] Lv, C.; Hu, C.; Luo, J. H.; Liu, S.; Qiao, Y.; Zhang, Z.; Song, J. F.; Shi, Y.; Cai, J. G.; Watanabe, A. Recent advances in graphene-based humidity sensors. *Nanomaterials* **2019**, *9*, 422.
[13] Lee, C. Y.; Lee, G. B. Humidity sensors: A review. *Sens. Lett.* **2005**, *3*, 1–15.
[14] Pacheco-Fernández, I.; Pino, V. Extraction with ionic liquids-organic compounds. In *Liquid-Phase Extraction*. Poole, C. F., Ed.; Elsevier: Amsterdam, 2020.
[15] Correia, D. M.; Fernandes, L. C.; Martins, P. M.; García-Astrain, C.; Costa, C. M.; Reguera, J.; Lanceros-Méndez, S. Ionic liquid-polymer composites: A new platform for multifunctional applications. *Adv. Funct. Mater.* **2020**, *30*, 1909736.
[16] Yang, Q. W.; Zhang, Z. Q.; Sun, X. G.; Hu, Y. S.; Xing, H. B.; Dai, S. Ionic liquids and derived materials for lithium and sodium batteries. *Chem. Soc. Rev.* **2018**, *47*, 2020–2064.
[17] Ye, Y. S.; Rick, J.; Hwang, B. J. Ionic liquid polymer electrolytes. *J. Mater. Chem. A* **2013**, *1*, 2719–2743.
[18] Watanabe, M.; Thomas, M. L.; Zhang, S. G.; Ueno, K.; Yasuda, T.; Dokko, K. Application of ionic liquids to energy storage and conversion materials and devices. *Chem. Rev.* **2017**, *117*, 7190–7239.
[19] Yin, L.; Li, S.; Liu, X. H.; Yan, T. Y. Ionic liquid electrolytes in electric double layer capacitors. *Sci. China Mater.* **2019**, *62*, 1537–1555.
[20] Ma, Z.; Yu, J. H.; Dai, S. Preparation of inorganic materials using ionic liquids. *Adv. Mater.* **2010**, *22*, 261–285.
[21] Olivier-Bourbigou, H.; Magna, L.; Morvan, D. Ionic liquids and catalysis: Recent progress from knowledge to applications. *Appl. Catal. A Gen.* **2010**, *373*, 1–56.
[22] Bhide, A.; Jagannath, B.; Graef, E.; Willis, R.; Prasad, S. Versatile duplex electrochemical sensor for the detection of CO_2 and relative humidity using room temperature ionic liquid. *ECS Trans.* **2018**, *85*, 751–765.
[23] Lee, J.; Emon, M. O. F.; Vatani, M.; Choi, J. W. Effect of degree of crosslinking and polymerization of 3D printable polymer/ionic liquid composites on performance of stretchable piezoresistive sensors. *Smart Mater. Struct.* **2017**, *26*, 035043.
[24] Lai, K. F.; Su, W. Y.; Chang, W. T.; Cheng, S. H. The synergic effect of conducting polymer/ionic liquid composite electrodes on the voltammetric sensing of biomolecules. *Int. J. Electrochem. Sci.* **2013**, *8*, 7959–7975.
[25] Widegren, J. A.; Magee, J. W. Density, Viscosity, speed of sound, and electrolytic conductivity for the ionic liquid 1-hexyl-3-methylimidazolium bis(trifluoromethylsulfonyl)imide and its mixtures with water. *J. Chem. Eng. Data* **2007**, *52*, 2331–2338.
[26] Ota, H.; Chen, K.; Lin, Y. J.; Kiriya, D.; Shiraki, H.; Yu, Z. B.; Ha, T. J.; Javey, A. Highly deformable liquid-state heterojunction sensors. *Nat. Commun.* **2014**, *5*, 5032.
[27] Xiao, S. H.; Nie, J. X.; Tan, R.; Duan, X. C.; Ma, J. M.; Li, Q. H.; Wang, T. H. Fast-response ionogel humidity sensor for real-time monitoring of breathing rate. *Mater. Chem. Front.* **2019**, *3*, 484–491.
[28] Wang, L. L.; Duan, X. C.; Xie, W. Y.; Li, Q. H.; Wang, T. H. Highly chemoresistive humidity sensing using poly(ionic liquid)s. *Chem. Commun.* **2016**, *52*, 8417–8419.
[29] Fernandes, L. C.; Correia, D. M.; Pereira, N.; Tubio, C. R.; Lanceros-Méndez, S. Highly sensitive humidity sensor based on ionic liquid-polymer composites. *ACS Appl. Polym. Mater.* **2019**, *1*, 2723–2730.
[30] Zhen, Z.; Li, Z. C.; Zhao, X. L.; Zhong, Y. J.; Zhang, L.; Chen, Q.; Yang, T. T.; Zhu, H. W. Formation of uniform water microdroplets on wrinkled graphene for ultrafast humidity sensing. *Small* **2018**, *14*, 1703848.
[31] Wu, J.; Wu, Z. X.; Tao, K.; Liu, C.; Yang, B. R.; Xie, X.; Lu, X. Rapid-response, reversible and flexible humidity sensing platform using a hydrophobic and porous substrate. *J. Mater. Chem. B* **2019**, *7*, 2063–2073.
[32] Bjorkqvist, M.; Paski, J.; Salonen, J.; Lehto, V. P. Studies on hysteresis reduction in thermally carbonized porous silicon humidity sensor. *IEEE Sens. J.* **2006**, *6*, 542–547.
[33] Kuang, Q.; Lao, C. S.; Wang, Z. L.; Xie, Z. X.; Zheng, L. S. High-sensitivity humidity sensor based on a single SnO_2 nanowire. *J. Am. Chem. Soc.* **2007**, *129*, 6070–6071.
[34] Kano, S.; Kim, K.; Fujii, M. Fast-response and flexible nanocrystal-based humidity sensor for monitoring human respiration and water evaporation on skin. *ACS Sens.* **2017**, *2*, 828–833.
[35] Mohd-Noor, S.; Jang, H.; Baek, K.; Pei, Y. R.; Alam, A. M.; Kim, Y. H.; Kim, I. S.; Choy, J. H.; Hyun, J. K. Ultrafast humidity-responsive structural colors from disordered nanoporous titania microspheres. *J. Mater. Chem. A* **2019**, *7*, 10561–10571.
[36] Borini, S.; White, R.; Wei, D.; Astley, M.; Haque, S.; Spigone, E.; Harris, N.; Kivioja, J.; Ryhanen, T. Ultrafast graphene oxide humidity sensors. *ACS Nano* **2013**, *7*, 11166–11173.
[37] Zhuang, Z.; Qi, D.; Ru, C. Y.; Pan, J.; Zhao, C. J.; Na, H. Fast response and highly sensitive humidity sensors based on $CaCl_2$-doped sulfonated poly (ether ether ketone)s. *Sens. Actuators B Chem.* **2017**, *253*, 666–676.
[38] Zhang, Z. Y.; Huang, J. D.; Yuan, Q.; Dong, B. Intercalated graphitic carbon nitride: A fascinating two-dimensional nanomaterial for an ultra-sensitive humidity nanosensor. *Nanoscale* **2014**, *6*, 9250–9256.
[39] Wei, Z. Q.; Zhou, Z. K.; Li, Q. Y.; Xue, J. C.; Di Falco, A.; Yang, Z. J.; Zhou, J. H.; Wang, X. H. Flexible nanowire cluster as a wearable colorimetric humidity sensor. *Small* **2017**, *13*, 1700109.
[40] Chi, H.; Liu, Y. J.; Wang, F. K.; He, C. B. Highly sensitive and fast response colorimetric humidity sensors based on graphene oxides film. *ACS Appl. Mater. Interfaces* **2015**, *7*, 19882–19886.
[41] Fernandes, L. C.; Correia, D. M.; Garcia-Astrain, C.; Pereira, N.; Tariq, M.; Esperança, J. M. S. S.; Lanceros-Méndez, S. Ionic-liquid-based printable materials for thermochromic and thermoresistive applications. *ACS Appl. Mater. Interfaces* **2019**, *11*, 20316–20324.
[42] Kim, K. W.; Oh, H.; Bae, J. H.; Kim, H.; Moon, H. C.; Kim, S. H. Electrostatic-force-assisted dispensing printing of electrochromic gels for low-voltage displays. *ACS Appl. Mater. Interfaces* **2017**, *9*, 18994–19000.
[43] Moon, H. C.; Lodge, T. P.; Frisbie, C. D. Solution processable, electrochromic ion gels for sub-1 V, flexible displays on plastic. *Chem. Mater.* **2015**, *27*, 1420–1425.